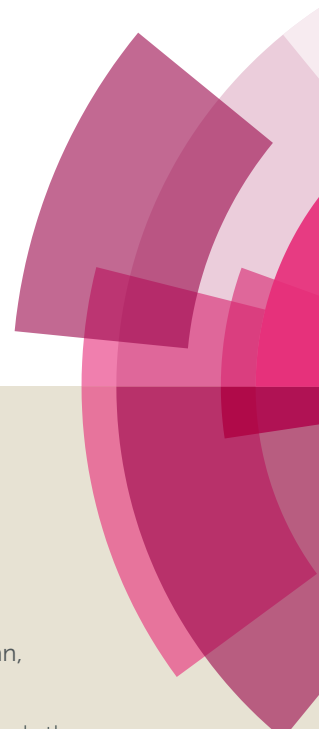


NJC

Accepted Manuscript



This article can be cited before page numbers have been issued, to do this please use: Z. Wang, X. Yuan, Q. Cheng, T. Zhang and J. Luo, *New J. Chem.*, 2018, DOI: 10.1039/C8NJ01934G.



This is an Accepted Manuscript, which has been through the Royal Society of Chemistry peer review process and has been accepted for publication.

Accepted Manuscripts are published online shortly after acceptance, before technical editing, formatting and proof reading. Using this free service, authors can make their results available to the community, in citable form, before we publish the edited article. We will replace this Accepted Manuscript with the edited and formatted Advance Article as soon as it is available.

You can find more information about Accepted Manuscripts in the [author guidelines](#).

Please note that technical editing may introduce minor changes to the text and/or graphics, which may alter content. The journal's standard [Terms & Conditions](#) and the ethical guidelines, outlined in our [author and reviewer resource centre](#), still apply. In no event shall the Royal Society of Chemistry be held responsible for any errors or omissions in this Accepted Manuscript or any consequences arising from the use of any information it contains.

COMMUNICATION

An efficient and recyclable acid-base bifunctional core-shell nano-catalyst for the one-pot deacetalization-Knoevenagel tandem reaction

Received 00th April 2018,
Accepted 00th January 20xx

DOI: 10.1039/x0xx00000x

www.rsc.org/

Zitao Wang[‡], Xiaofeng Yuan[‡], Qi'an Cheng, Tichun Zhang and Jun Luo*

A novel magnetic nanoparticle supported acid-base bifunctional catalyst was synthesized by anchoring [3-(2-aminoethyl)aminopropyl]triethoxysilane and sulfonic acid successively onto the surface of silica-coated Fe₃O₄ nanoparticles. The as-prepared nanoparticle was used as a “quasi-homogeneous” and recyclable catalyst for the one-pot deacetalization-Knoevenagel tandem reaction of benzaldehyde dimethylacetals and malononitrile. It shows high catalytic activity because the reaction proceeded smoothly and afforded benzylidenemalononitriles with excellent yields. Besides, it shows synergistic effect and facilitates the mass transfer process during the tandem reaction because the two catalytic moieties were connected together on the same MNP. Moreover, the catalyst can be readily recovered under the external magnetic field and reused without any significant loss of catalytic activity after six runs.

Introduction

The separation and purification of organic intermediates from reaction mixtures containing homogeneous catalysts generally are confronted with tedious workup procedure and more or less loss of total yield, especially in multistep synthesis^[1]. The application of multifunctional catalysts in multistep one-pot reactions can overcome the above problems because this protocol can reduce the separation step of intermediate products or show synergistic effect^[2-8]. It is generally known that more than 85% organic reactions involve catalysis, and the use of acid or base as catalysts is pretty common in the catalytic reactions^[9-12]. For a large number of multistep reactions, both acid and base are simultaneously needed. However, it is not easy to synthesize hostile groups on solid catalysts^[13]. Moreover, the examples of acid and base co-supported catalysts are limited.

Bifunctional catalysts have attracted intensive interests in recent years^[14-17]. For example, Wang and co-workers prepared a porous palladium-acid bifunctional nano-catalyst and used it in the one-pot synthesis of methyl isobutyl ketone from acetone^[18]. Rothenberg and co-workers added different amounts of heteropoly acid to the aminopropylsilica to prepare acid-base bifunctional supported catalyst and used it

to catalyse deacetalization-Henry tandem reactions of benzaldehyde derived acetals^[19]. Rana reported the deacetalization-Knoevenagel tandem reaction catalysed by a silica gel supported sulfonic acid and amine bifunctional catalyst^[20]. Zhao et al. used ortho aminophene terephthalic acid and Zinc nitrate to prepare a metal organic framework encapsulated palladium nanoparticle and applied it as a primary amine and palladium bifunctional catalyst^[21]. Li et al. deposited palladium nanoparticles on the surface of aminopropyl functionalized nano iron oxide and applied it to catalyse the Knoevenagel condensation and hydrogenation cascade reactions of aromatic aldehydes and malononitrile in one pot with almost quantitative yield^[22].

Magnetic nanoparticle (MNP) supported catalysts, as the ideal alternative of homogeneous and classical heterogeneous catalysts, have attracted broad attention.^[23-30] MNPs generally have high specific surface areas so that high loading ratio of catalyst is predictable. In comparison with common solid carriers, MNPs can disperse thoroughly in the reaction mixture so as to show “quasi-homogeneous” property. At the same time, MNPs also has the advantages of easy recovery by external magnetic field and diverse surface decoration.^[31-35] Compared with other magnetic nanoparticles, nano-Fe₃O₄ has some attractive advantages including very low price, extra fineness and easy functionalization, so it is widely applied in the fields of nanotechnology, biological applications^[36-37], pollution control^[38] and catalysis^[39-43].

For the catalysts used in one-pot tandem reactions, the catalytic moieties of bifunctional catalysts are basically on the solid surface, however, this kind of nanoscale catalysts are few in literatures. That is, most of the supported bifunctional catalysts belong to the conventional heterogeneous catalysis.

School of Chemical Engineering, Nanjing University of Science and Technology, Nanjing 210094, China.

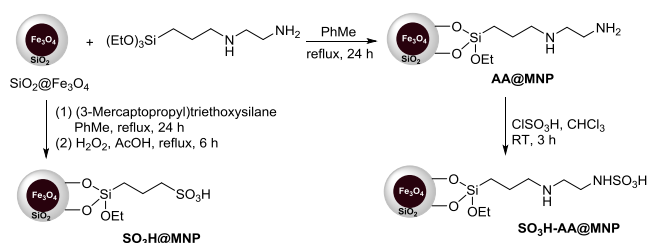
E-mail: luojun@njut.edu.cn;

[†] Electronic Supplementary Information (ESI) available: [details of any supplementary information available should be included here]. See DOI: 10.1039/x0xx00000x

[‡] These authors contributed equally to this work and should be considered co-first authors.

Compared with the reported stepwise catalytic activity of the dual functional catalysts and the single functional catalysts, the bifunctional catalyst has no obvious promoting effect on the catalytic activity between different catalytic centers, and each plays independent catalytic roles in the tandem reactions.

Herein, we report an efficient and magnetically recoverable sulfonic acid and secondary amine bifunctional core-shell nano-catalyst, Scheme 1, and used it as a “quasi-homogeneous” and recyclable catalyst for the one-pot deacetalization-Knoevenagel tandem reaction of benzaldehyde dimethylacetals and malononitrile.



Scheme 1. Synthetic route to acid and base monofunctional and bifunctional NMPs.

Results and Discussion

The acid-base bifunctional catalyst $\text{SO}_3\text{H-AA@MNP}$ was prepared *via* the two-step procedure demonstrated in Scheme 1. Firstly, a condensation reaction of $\text{SiO}_2@\text{Fe}_3\text{O}_4$ with 3-(2-aminoethyl)aminopropyltrimethoxysilane afforded amine-functionalized MNP (AA@MNP). Subsequently, AA@MNP was reacted with chlorosulfonic acid in chloroform at room temperature for 3 h to afford the target bifunctional catalyst $\text{SO}_3\text{H-AA@MNP}$. The loading amount of the organic moiety was determined to be $0.75 \text{ mmol} \cdot \text{g}^{-1}$ by elemental analysis, which was also supported by TG analysis (see Supplementary information).

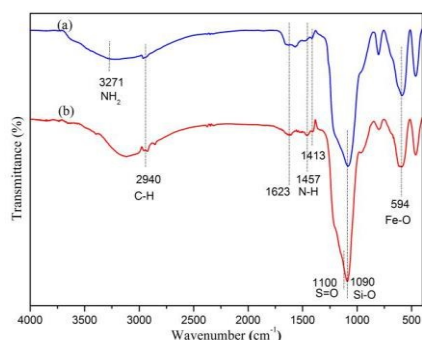


Figure 1. FTIR spectra for (a) AA@MNP (blue line) and (b) $\text{SO}_3\text{H-AA@MNP}$ (red line).

The FTIR spectroscopy was used to characterize the composition of $\text{SO}_3\text{H-AA@MNP}$ nanoparticles. As shown in

Fig.1, the relatively high intensity of a band at 594 cm^{-1} is characteristic of the Fe-O stretching vibrations, which indicates the high content of Fe_3O_4 nanoparticles. Meanwhile, the Si-O-Si stretching modes of the silica shell can be observed as a strong peak at around 1090 cm^{-1} , which shows the existence of silicon film. The signal at about $1,100 \text{ cm}^{-1}$ is due to S=O stretching vibration of sulfonic acid motif. The small peak at the 2940 cm^{-1} band proves the presence of the CH_2 group. The band at 1413 cm^{-1} is assigned to the asymmetric stretching of SO_2 moiety and a band at 1623 cm^{-1} belongs to sulfonic OH deformation vibration, which can confirm the existence of sulfonic acid. Meanwhile, the peaks between 1400 cm^{-1} and 1600 cm^{-1} correspond to the deformation mode of extracted R_2NH , hydrogen-bonded R_2NH and R_2NH_2^+ ^[44]. Therefore, the extra peak at 1457 cm^{-1} could be considered as an amine group, which is also confirmed by the NH_2 peak near 3300 cm^{-1} . These characteristic peaks in the FTIR could prove that the $\text{SiO}_2@\text{Fe}_3\text{O}_4$ nanoparticles were successfully immobilized with sulfonic acid and secondary amine moieties conjointly.

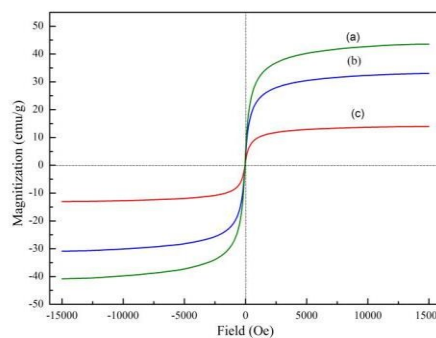


Figure 2. Room-temperature magnetization curves of (a) $\text{SiO}_2@\text{Fe}_3\text{O}_4$ (green line), (b) AA@MNP (blue line) and (c) $\text{SO}_3\text{H-AA@MNP}$ (red line).

The magnetic behaviour of the sample was measured at room temperature within the range of -15000 to 15000 Oe magnetic field by using a vibrating sample magnetometer (VSM). As shown in Figure 2, the magnetic properties of the three samples reach saturation in 1.5 T magnetic field, and the maximum magnetic saturation strengths of Fe_3O_4 , AA@MNP and $\text{SO}_3\text{H-AA@MNP}$ are 43.55 , 32.97 and $13.93 \text{ emu} \cdot \text{g}^{-1}$ respectively. The decrease of the saturation magnetization is due to the decrease of the iron oxide content in the sample, which proves the existence of silica in the core-shell structured materials. Meanwhile, the magnetization intensity of $\text{SiO}_2@\text{Fe}_3\text{O}_4$ immobilized with SO_3H group is much lower than that of bare $\text{SiO}_2@\text{Fe}_3\text{O}_4$ nanoparticles, and the decrease of saturation magnetization may be related to the presence of sulfonic group. In addition, all the magnetization curves pass through the zero point, so there is no hysteresis, indicating that all the three nanoparticles are superparamagnetic. Once the external magnetic field is removed, the as-prepared catalyst has no residual magnetism, which facilitates the recovery of the catalyst. As shown in Figure 3(a), the catalyst

can be uniform dispersed in the solution by shaking or ultrasonic irradiation, which results in the “quasi-homogeneous” phenomenon. Meanwhile, $\text{SO}_3\text{H-AA@MNP}$ can be quickly collected in a few seconds in the external magnetic field to make the solution clear (Figure 3(b)).

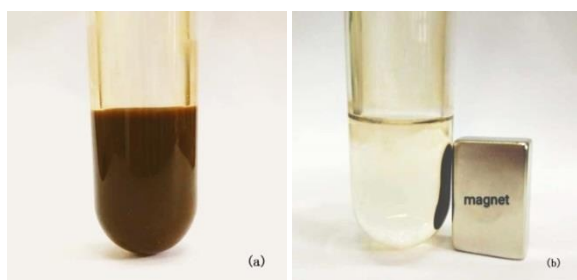


Figure 3. $\text{SO}_3\text{H-AA@MNP}$ is (a) dispersed well in the reaction system and (b) separated simply from the reaction system using an external magnet.

The morphology of the catalyst was analysed by TEM. As shown in Figure 4(a), the dark nano- Fe_3O_4 cores are surrounded by grey silica shell of about 3-5 nm thick and the size of the obtained catalyst falls in the range of 20-30 nm. Moreover, the nanoparticles are well dispersed. Figure 4(b) shows the recovered catalyst after reused in model reaction for six times. There is almost no apparent change in its morphology can be observed. In other words, the as-prepared supported bifunctional nano-catalyst has excellent chemical stability for the deacetalization-Knoevenagel tandem reaction.

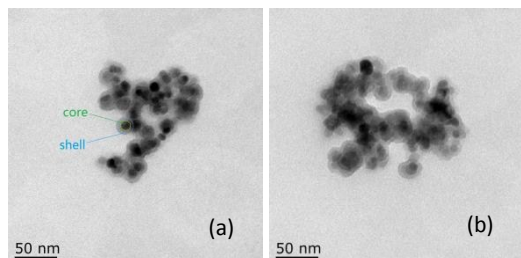


Figure 4. TEM images of fresh catalyst (a) recycled catalyst after six runs (b).

The surface composition of $\text{SO}_3\text{H-AA@MNP}$ was analysed with XPS. As shown in Fig. 5(a), the peaks with binding energy at 25.9, 103.0, 154.8, 169.0, 232.1, 285.4, 402.2 and 532.1 eV are distributed to O 2s, Si 2p, Si 2s, S 2p, S 2s, C 1s, N 1s and O 1s, which affirms that the catalyst is made up of C, O, Si, S and N in the survey scan of $\text{SO}_3\text{H-AA@MNP}$. The peaks with binding energy at 711 and 724 eV are distributed to Fe $2p_{1/2}$ and Fe $2p_{3/2}$, which also affirms that the catalyst contains Fe. The peaks with binding energy at 711 and 724 eV are weak, attributing to the fact that the Fe_3O_4 nanoparticles are surrounded by silica shell, which is in accordance with the FTIR and TEM results discussed previously. The O 1s components centered at 529.8, 531.6 and 532.7 eV, which correspond to Fe-O, S=O and Si-O, respectively (Fig. 6(b))^[45]. In the N 1s spectrum of $\text{SO}_3\text{H-AA@MNP}$, the component peaks at 401.6 eV and 399.6 eV are attributed to the C-N and C-N-C bonds,

respectively (Fig. 6(c))^[46]. $\text{SO}_3\text{H-AA@MNP}$ displays a peak at 168.6 eV associated with a S-O bond (Fig. 6(d)). As mentioned previously, IR spectroscopy shows that as-prepared catalyst has S=O bond. The XPS test further confirms the presence of S element in $\text{SO}_3\text{H-AA@MNP}$.

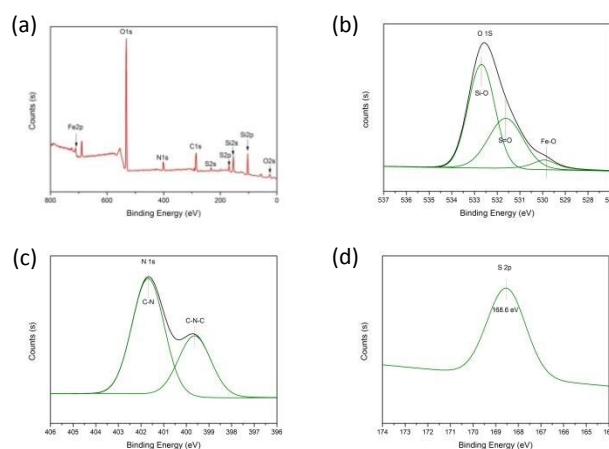


Figure 5. XPS spectra of $\text{SO}_3\text{H-AA@MNP}$. (a) Survey scan, (b) O 1s, (c) N 1s and (d) S 2p.

X-ray diffraction (XRD) is an effective method for the analysis of the composition and structure of solid materials. Figure 6 shows the high-angle XRD patterns of $\text{SiO}_2@\text{Fe}_3\text{O}_4$, AA@MNP, and $\text{SO}_3\text{H-AA@MNP}$. The wide peak at $2\theta=20\sim 30^\circ$ can be attributed to the amorphous silica layer of the outer layer. The diffraction peaks (220), (311), (400), (422), (511) and (440) are attributed to the standard Fe_3O_4 sample (JCPDS file no. 19-0629). It can be concluded that the surface modification of Fe_3O_4 does not lead to phase transition.

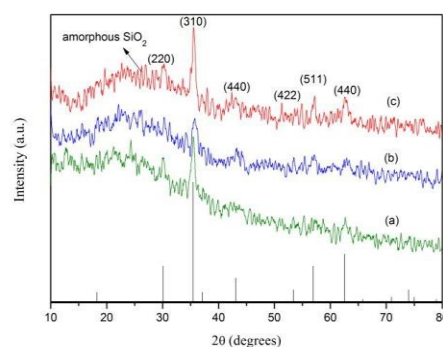
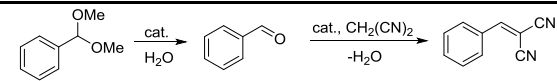


Figure 6. XRD patterns of (a) $\text{SiO}_2@\text{Fe}_3\text{O}_4$ (green line), (b) AA@MNP (blue line) and (c) $\text{SO}_3\text{H-AA@MNP}$ (red line).

The activity of the novel catalyst was tested using the one-pot deacetalization-Knoevenagel tandem reaction of benzaldehyde dimethylacetal (2 mmol) and malononitrile (2.1 mmol) as model substrates under nitrogen atmosphere and the results are listed in Table 1.

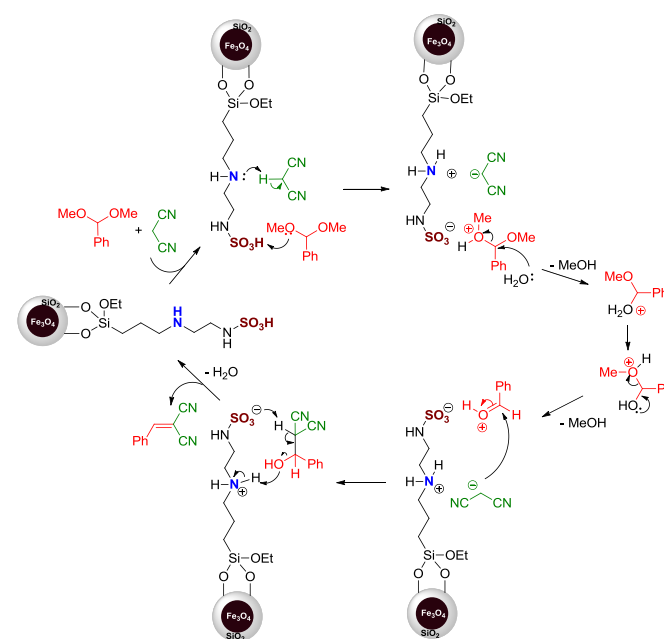
Table 1 Optimization of the reaction conditions^a


Entry	Catalyst (mg)	Solvent	Temp. (°C)	Time (h)	Yield (%) ^b
1	SO ₃ H-AA@MNP (20)	EtOH	reflux	2	87
2	SO ₃ H-AA@MNP (20)	H ₂ O	reflux	2	54
3	SO ₃ H-AA@MNP (20)	DMF	90	2	91
4	SO ₃ H-AA@MNP (20)	Toluene	90	2	94
5	—	Toluene	90	2	trace
6	SO ₃ H-AA@MNP (5)	Toluene	90	2	81
7	SO ₃ H-AA@MNP (10)	Toluene	90	2	89
8	SO ₃ H-AA@MNP (30)	Toluene	90	2	94
9	SO ₃ H-AA@MNP (20)	Toluene	70	2	86
10	SO ₃ H-AA@MNP (20)	Toluene	50	2	83
11	AMSA-MIL-101-NH ₂ ^[6]	Toluene	90	10	>99 ^c
12	DL-COF-1 ^[2]	CDCl ₃	RT	20	98 ^d
13	SiO ₂ @Fe ₃ O ₄ (20)	Toluene	90	2	trace
14	SO ₃ H@MNP (20)	Toluene	90	2	97 ^e
15	AA@MNP (20)	Toluene	90	2	90 ^f
16	SO ₃ H@MNP (20) & AA@MNP (20)	Toluene	90	2	88

^a Reaction conditions: benzaldehyde dimethylacetal (2 mmol), malononitrile (2.1 mmol), SO₃H-AA@MNP, H₂O (0.2 mmol) and solvent (20 mL). ^b GC yields. ^c A mixture of benzaldehyde dimethylacetal (0.76 g, 5 mmol), malononitrile (0.40 g, 6 mmol), AMSA-MIL-101-NH₂ (0.08 g, 10 wt%), anhydrous toluene (10 mL), 363 K, 10 h. ^d benzaldehyde dimethylacetal (1 mmol), malononitrile (1 mmol), DL-COF-1 (10 mol%), CDCl₃ (3 mL), RT, 20 h. ^e the yield of deacetalization product benzaldehyde; ^f the yield of Knoevenagel condensation of benzaldehyde and malononitrile.

The effect of some commonly used solvents including ethanol, water, N,N-dimethylformamide (DMF) and toluene was first tested (Table 1, entries 1-4). As shown in Table 1, toluene is the best choice since it gives the highest yield (Table 1, entry 4) while water is the worst one. So toluene was used in the subsequent investigations. The yield ascends with the increase of catalyst amount (Table 1, entries 4-8). In the absence of catalyst, almost no product can be detected (Table 1, entry 5). However, when the catalyst amount was above 20 mg, the yield remains unchanged (Table 1, entry 8). So the reaction conditions of entry 4 were applied as the standard conditions for the subsequent study. Lower yields were observed when the reaction temperature was reduced to 70 °C and 50 °C (Table 1, entries 9 and 10). Compared with the catalysts studied by scientists in recent years^[2,6], the as-prepared catalyst shows higher catalytic activity because similar yields are achieved but the reaction time is much shorter (Table 1, entries 11 and 12). To better show why the catalyst has so high catalytic activity, some control experiments were studied. There are some free Si-OH remains on the surface of SiO₂@Fe₃O₄, but it showed no catalytic activity in this reaction (Table 1, entry 13). The acid mono-

functionalized catalyst SO₃H@MNP was used but only the deacetalization product benzaldehyde was obtained with 97% yield, and no Knoevenagel condensation product was detected (Table 1, entry 14). As a contrast, the amine functionalized catalyst AA@MNP could efficiently catalyzed the Knoevenagel condensation of benzaldehyde and malononitrile under the standard reaction conditions and afford 2-benzylidenemalononitrile in 90% yield, which is slightly lower than the SO₃H-AA@MNP catalyzed one-pot deacetalization–Knoevenagel tandem reaction (Table 1, entry 15). It is notable that the combined use of the two solely functionalized catalysts AA@MNP and SO₃H@MNP in the tandem reaction resulted in 88% yield, which is obviously lower than the bifunctional catalyst. The reason was assigned to the more efficient mass transfer process when the MNP supported bifunctional catalyst, in which two catalytic moieties were connected together, was used.

**Scheme 2.** Proposed mechanism of the one-pot deacetalization-Knoevenagel tandem reaction catalysed by SO₃H-AA@MNP.

A cooperative mechanism of the one-pot deacetalization-Knoevenagel reaction catalysed by SO₃H-AA@MNP was proposed and depicted in Scheme 2. The reaction sequences involve two steps as follows: The first step is an acid-catalysed deacetalization and the subsequent step is a base-catalysed C-C bond formation. In other words, the benzaldehyde dimethylacetal is activated by the sulfonic acid moiety to form oxonium ion. At the same time, active α-H of malonitrile is captured by the secondary amine moiety. Then the protonated oxonium ion is attacked by water and release methanol to afford protonated benzaldehyde. Subsequently, the activated carbonyl of aldehyde undergoes nucleophilic attack by malonitrile carbanion. At last, a synergistic dehydration occurs to produce the final product 2-benzylidenemalononitrile and regenerate the catalyst.

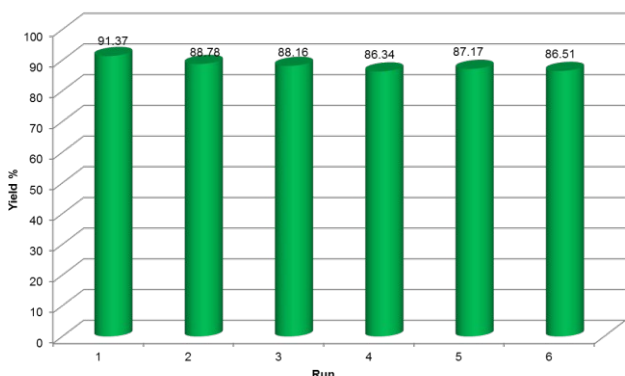
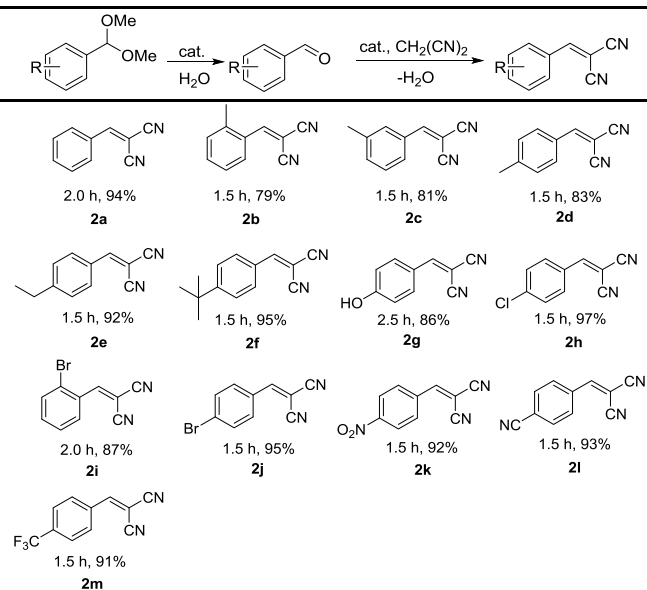


Figure 7. Recycling results of SO₃H-AA@MNP.

The recovery and reuse of a catalyst is highly preferable for a green process. Thus, the recyclability of SO₃H-AA@MNP was investigated by using benzaldehyde dimethylacetal and malononitrile as model substrates. The catalyst was easily separated by attaching an external magnet after the reaction. The reclaimed catalyst was washed with ethyl acetate, dried under vacuum and reused in subsequent reactions. As shown in Figure 7, the results show that the catalytic activity of the catalyst has no obvious loss within six runs. Furthermore, the TEM image demonstrated in Figure 4(b) indicates the morphology of the recovered catalyst remains unchanged. The above results show that the catalyst is tolerable to the one-pot deacetalization-Knoevenagel tandem reaction and exhibits excellent chemical stability.

Table 2 SO₃H-AA@MNP catalysed one-pot deacetalization-Knoevenagel tandem reactions^a



^a Reaction conditions: benzaldehyde dimethylacetals (2 mmol), malononitrile (2.1 mmol), toluene (20 mL), SO₃H-AA@MNP (20 mg), H₂O (22 mmol), 90 °C.

The generality of this catalyst was evaluated by using various acetals and malononitrile as substrates and performing the reaction under the optimized reaction conditions. The collected results are listed in Table 2. As shown in Table 2, benzaldehyde dimethylacetal with electron-withdrawing or electron-donating groups underwent efficient coupling with malononitrile at 90 °C for 1.5–2.5 h to afford the corresponding substituted benzylidenemalononitriles in good to excellent yields ranging from 74% to 97% (Table 2, entries 1–13). However, electron-donating groups such as alkyl and hydroxyl are unfavorable to the reaction in comparison to electron-withdrawing ones including nitro, chlorine, bromine, trifluoromethyl and cyano functionalities. In addition, steric hindrance obviously influences the reaction, which can be seen from a comparison of the results for methylbenzaldehyde acetal (Table 2, entries 2–4) and bromobenzaldehyde acetal (Table 2, entries 9 and 10). Because the vicinal steric effect is greater than the contrapuntal one, 4-substituted benzaldehyde acetals show higher reactivity than 2-substituted isomers.

Conclusions

In summary, secondary amine and sulfonic acid were sequentially immobilized on the surface of silica-coated Fe₃O₄ nanoparticle to afford an acid-base bifunctional magnetic nano-catalyst SO₃H-AA@MNP, which was used as a recyclable catalyst for the one-pot deacetalization-Knoevenagel reaction of benzaldehyde dimethylacetals and malononitrile. It showed high catalytic activity because the reaction proceeded smoothly and afforded benzylidenemalononitriles with high to excellent yields. Because the two catalytic moieties were connected together on the same MNP, a possible reaction mechanism involving a co-operative action of acid and base, which can facilitate the mass transfer process during the tandem reaction, was established. Besides, the catalyst can be readily recovered under external magnetic field, and reused without any significant loss of catalytic activity after six runs.

Experimental section

General information

The IR spectra were recorded on a Nicolet spectrometer (KBr). ¹H NMR and ¹³C NMR spectra were recorded on a Bruker Avance-III DRX spectrometer operating at 500 MHz and 125 MHz respectively, using CDCl₃ as solvent. X-ray diffraction (XRD) images were obtained from a Bruker XRD D8 Advance instrument with Cu Kα radiation (λ = 0.15418 nm). Transmission electron microscopy (TEM) images were obtained using a JEM-2100 instrument. The magnetization curve was obtained by a vibrating sample magnetometer (JDM-13T, China). Elemental analysis was performed with an Elementar Vario EL 6 recorder. X-ray photoelectron spectroscopy (XPS) spectra were obtained from an ESCALAB™ 250Xi instrument. All the solvents used were strictly dried

according to standard operation and stored on 4 Å molecular sieves. All other chemicals (AR grade) were commercially available and used without further purification. Silica-coated Fe₃O₄ nanoparticle (SiO₂@Fe₃O₄) was prepared according to reported procedure^[25].

Synthesis of amine-functionalized MNP (AA@MNP)

SiO₂@Fe₃O₄ (0.2 g) was dispersed in dry toluene (20 mL) by sonication for 0.5 h, [3-(2-aminoethyl)aminopropyl]triethoxysilane (1.32 g, 5 mmol) was added and the reaction mixture was refluxed for 24 h under nitrogen atmosphere. After being cooled to ambient temperature, the amine-functionalized MNP was collected by a permanent magnet and washed thoroughly with toluene and acetone successively, then dried under vacuum overnight.

Synthesis of acid-base bifunctional MNP (SO₃H-AA@MNP)

A mixture of AA@MNP (0.2 g), ClSO₃H (1 mmol 0.07 mL) and chloroform (20 mL) was stirred at room temperature for 3 h. The acid-base functional MNPs were collected by a permanent magnet and washed thoroughly with dichloromethane (3 × 5 mL), and then dried under vacuum overnight. The loading content of the organic moiety was determined to be 0.75 mmol·g⁻¹ by elemental analysis.

General procedure for SO₃H-AA@MNP catalysed one-pot deacetalization–Knoevenagel tandem reaction

A mixture of benzaldehyde dimethylacetal (2 mmol), malononitrile (2.1 mmol), SO₃H-AA@MNP (20 mg), H₂O (0.2 mmol) and toluene (20 mL) was stirred at 90 °C under nitrogen atmosphere for 2 h. The solid catalyst was recovered using a permanent magnet, and the filtrate was dried over anhydrous sodium sulfate and evaporated under reduced pressure to afford the product. The crude product was purified by column chromatography on silica gel to give the pure product.

Conflicts of interest

There are no conflicts to declare.

Acknowledgements

This work was sponsored by the Natural Science Foundation of Jiangsu Province of China (no. BK2010485) and Qing Lan Project of Jiangsu Province, P. R. China.

Notes and references

- L. Shiri, S. Zarei, M. Kazemi and D. Sheikh. *Appl Organometal Chem*, 2018, e3938.
- H. Li, Q. Pan, Y. Ma, X. Guah, M. Xue, Q. fang, Y. Yan, V. Valtchev and S. Qiu. *J. Am. Chem. Soc.*, 2016, 138, 14783-14788.
- E. Merino, E. Verdesesto, E. M. Maya, M. Iglesias, F. Sánchez, and A. Corma. *Chem. Mater.*, 2013, 25, 981-988.
- F. Wei, J. Liu, Y. N. Zhu, X. S. Wang, C. Y. Cao and W. G. Song. *Sci. China Chem.*, 2017, 60, 1236-1242.
- Y. Zhang, B. Li, S. Ma. *Chem. Commun.*, 2014, 50, 8507-8510.

- M. Mu, X. Yan, Y. Li and L. Chen. *J. Nanopart. Res.*, 2017, 19(12), 1-9. View Article Online
DOI: 10.1039/C8NJ01934G
- E. Gianotti, U. Diaz, A. Veltva and A. Corma. *Catal. Sci. Technol.*, 2013, 3, 2677-2688.
- S Rostamizadeh, A Hemmasi and N Zekri. *Nanochem. Res.*, 2017, 2, 29-41.
- K. K. Sharma and T. Asefa. *Angew. Chem. Int. Ed.*, 2007, 46, 2879-2882.
- S. Shylesh, A. Wagener, A. Seifert, S. Ernst and W. R. Thiel. *Angew. Chem. Int. Ed.*, 2010, 49, 184-187.
- E. L. Margelefsky, R. K. Zeidan, V. Dufaud and M. E. Davis. *J. Am. Chem. Soc.*, 2007, 129, 13691-13697.
- E. L. Margelefsky, A. Bendjériou, R. K. Zeidan, V. Dufaud and M. E. Davis. *J. Am. Chem. Soc.*, 2008, 130, 13442-13449.
- N. R. Shiju, A. H. Alberts, S. Khalid, D. R. Brown and G. Rothenberg. *Angew. Chem. Int. Ed.*, 2011, 50, 9615-9619.
- M. Mu, X. Yan, Y. Li and L. Chen. *J. Nanopart. Res.*, 2017, 19, 148.
- F. Zhang, H. Jiang, X. Li, X. Wu and H. Li. *ACS Catal.*, 2014, 4, 394-401.
- C. You, C. Yu, X. Yang, Y. Li, H. Huo, Z. Wang, Y. Jiang, X. Xu and K. Lin. *New J. Chem.*, 2018, 42, 4095-4101.
- L. Xiong, H. Zhang, Z. He, T. Wang, Y. Xu, M. Zhou and K. Huang. *New J. Chem.*, 2018, 42, 1368-1372.
- P. Wang, S. Y. Ba, J. Zhao, P. Su, Q. Yang and C. Li. *ChemSusChem*, 2012, 5, 2390-2396.
- N. R. Shiju, A. H. Alberts, S. Khalid, D. R. Brown and G. Rothenberg. *Angew. Chem. Int. Ed.*, 2011, 50, 9615-9619.
- S. Rana, S. Maddila, R. Pagadala and S. B. Jonnalagadda. *J. Porous Mater.*, 2015, 22, 353-360.
- M. Zhao, K. Deng, L. He, Y. Liu, G. Li, H. Zhao and Z. Tang. *J. Am. Chem. Soc.*, 2014, 136, 1738-1741.
- P. Li, Y. Yu, H. Liu, C. Y. Cao and W. G. Song. *Nanoscale*, 2014, 6, 442-448.
- R. B. N. Baig and R. S. Varma. *Chem. Commun.*, 2013, 49, 752-770.
- V. Polshettiwar, R. Luque, A. Fihri, H. Zhu, M. Bouhrara and J. M. Basset. *Chem. Rev.*, 2011, 111, 3036-3075.
- Q. Zhang, H. Su, J. Luo and Y. Wei. *Green Chem.*, 2012, 14, 201-208.
- Q. Zhang, H. Su, J. Luo and Y. Wei. *Catal. Sci. Tech.*, 2013, 3, 235-243
- Q. Zhang, H. Su, J. Luo and Y. Wei. *Tetrahedron*, 2013, 69, 447-454.
- S. Rezaei, A. Ghorbani-Choghamarani, R. Badri and A. Nikseresht. *Appl. Organometal. Chem.*, 2017, 32, e3948.
- L. Shiri and B. Tahmasbi. *Phosphorus Sulfur*, 2017, 192, 53-57.
- B. Wang, L. Si, J. Geng, Y. Su, Y. Li, X. Yan and L. Chen. *Appl. Catal. B-Environ.*, 2017, 204, 316-323.
- L. Zhang, P. Li, C. Liu, J. Yang, M. Wang and L. Wang. *Catal. Sci. Technol.*, 2014, 4, 1979-1988.
- L. Shiri, A. Ghorbani-Choghamarani and M. Kazemi. *Appl. Organometal. Chem.* 2017, 31, e3596.
- P. Wang, A. G. Kong, W. J. Wang, H. Y. Zhu and Y. K. Shan. *Catal. Lett.*, 2010, 135, 159-164.
- Y. Zhanga, Y. Zhao and C. Xia. *J. Mol. Catal. A: Chem.*, 2009, 306, 107-112.
- Q. Deng, Y. Shen, H. Zhu and T. Tu. *Chem. Commun.*, 2017, 53, 13063-13066.
- Y. Yong, R. Su, X. Liu, W. Xua, Y. Zhang, R. Wang, P. Ouyang, J. Wu, J. Ge and Z. Liua. *Biochem. Eng. J.*, 2018, 129, 26-32.
- Y. T. Wang, Z. Fang and X. X. Yang. *Appl. Energy*, 2017, 204, 702-714.
- S. P. Yeap, J. Lim, B. S. Ooi and A. L. Ahmad. *J. Nanopart. Res.*, 2017, 19(11), 1-15.
- R. Hajian and A. Ehsanikhah. *Chem. Phys. Lett.*, 2018, 691, 146-154.

- 40 W. Gu, X. Deng, X. Jia, J. Li and E. Wang. *J. Mater. Chem. A*, 2015, 3, 8793-8799.
- 41 Z. S. Wu, S. Yang, Y. Sun, K. Parvez, X. Feng and K. Müllen. *J. Am. Chem. Soc.*, 2012, 134, 9082-9085.
- 42 Q. Yue, Y. Zhang, Y. Jiang, J. Li, H. Zhang, C. Yu, A. A. Elzatahry, A. Alghamdi, Y. Deng and D. Zhao. *J. Am. Chem. Soc.*, 2017, 139, 4954-4961.
- 43 Q. Yue, J. Li, Y. Zhang, X. Cheng, X. Chen, P. Pan, J. Su, A. A. Elzatahry, A. Alghamdi, Y. Deng and D. Zhao. *J. Am. Chem. Soc.*, 2017, 139, 15486-15493.
- 44 A. Walcarius, N. Luthi, J. L. Blin, B. L. Su and L. Lamberts. *Electrochim. Acta*, 1999, 44, 4601-4610.
- 45 M. Zhu, W. Zhang, Y. Li, L. Gai, J. Zhou and W. Maa. *J. Mater. Chem. A*, 2016, 4, 19060-19069.
- 46 Q. Du, T. Chen, J. Liu and X. Zeng. *Appl. Surf. Sci.*, 2018, 434, 588-595.
- 47 F. Liu, J. Sun, L. Zhu, X. Meng, C. Qi and F. S. Xiao. *J. Mater. Chem.*, 2012, 22, 5495-5502.

View Article Online
DOI: 10.1039/C8NJ01934G

Table of Contents:

An acid-base bifunctional nano-catalyst was synthesized and applied as efficient and recoverable catalyst in the one-pot deacetalization-Knoevenagel tandem reaction.

